

In situ Control of Si/Ge Growth on Stripe-Patterned Substrates Using Reflection High-Energy Electron Diffraction and Scanning Tunneling Microscopy

B. Sanduijav · D. G. Matei · G. Springholz

Received: 9 July 2010/Accepted: 17 September 2010/Published online: 6 October 2010
© The Author(s) 2010. This article is published with open access at Springerlink.com

Abstract Si and Ge growth on the stripe-patterned Si (001) substrates is studied using *in situ* reflection high-energy electron diffraction (RHEED) and scanning tunneling microscopy (STM). During Si buffer growth, the evolution of RHEED patterns reveals a rapid change of the stripe morphology from a multifaceted “U” to a single-faceted “V” geometry with {119} sidewall facets. This allows to control the pattern morphology and to stop Si buffer growth once a well-defined stripe geometry is formed. Subsequent Ge growth on “V”-shaped stripes was performed at two different temperatures of 520 and 600°C. At low temperature of 520°C, pronounced sidewall ripples are formed at a critical coverage of 4.1 monolayers as revealed by the appearance of splitted diffraction streaks in RHEED. At 600°C, the ripple onset is shifted toward higher coverages, and at 5.2 monolayers dome islands are formed at the bottom of the stripes. These observations are in excellent agreement with STM images recorded at different Ge coverages. Therefore, RHEED is an efficient tool for *in situ* control of the growth process on stripe-patterned substrate templates. The comparison of the results obtained at different temperature reveals the importance of kinetics on the island formation process on patterned substrates.

Keywords Quantum dots · Silicon · Germanium · Molecular beam epitaxy · Patterned substrates · Reflection

high-energy electron diffraction · Scanning tunneling microscopy

Introduction

Self-assembled growth of Stranski–Krastanow islands on pre-patterned substrates has attracted great interest [1–20] because it provides an effective route for positioning of quantum dots in nano-electronic devices. For patterning, various methods such as optical [1–3], holographic [4–7], electron beam [5–10], focused ion beam [12–14] as well as extreme UV interference lithography [15, 16] have been used, and different pattern geometries, including stripes [1, 4–6], mesas [2], and pits with various sizes and shapes [3, 7–17], have been employed. For site-control of deposited quantum dots, however, the pattern morphology has to be tightly controlled and the growth conditions tuned to the given template structure [5–17]. In particular, perfect site-control can be achieved only in a limited window of growth conditions [7, 12–17]. In addition, the shape of the pattern morphology as well as the growth conditions also determines where the quantum dots are formed on the surface. Under different conditions, thus, dot formation was found to occur at different substrate locations, such as in the center of pits [7–17], in the middle of grooves [4–6], at sidewalls [4–6], or even at edges or ridges [1, 2, 10, 12, 15, 16] of the pattern structures. Further complications arise from the limited thermal budget available for substrate treatment before epitaxial growth to preserve the pattern on the surface. Therefore, a buffer layer growth is required to remove the defects produced by the patterning process. During buffer growth, however, the pattern morphology rapidly changes and usually a complex multifaceted surface topography is formed [3–6, 15, 16], which further

B. Sanduijav · D. G. Matei · G. Springholz (✉)
Institut für Halbleiterphysik, Johannes Kepler University,
4040 Linz, Austria
e-mail: gunther.springholz@jku.at

Present Address:
D. G. Matei
University of Bielefeld, 33501 Bielefeld, Germany

modifies the dot nucleation process. Therefore, the whole process sequence must be tightly controlled for reproducible position control of the quantum dots.

In the present work, we report on *in situ* control of Si and Ge growth on stripe-patterned Si (001) substrates using reflection high-energy electron diffraction (RHEED) and scanning tunneling microscopy (STM) where large area patterns were produced by holographic lithography. Because of the simple geometry, stripes represent a model system [4–6] for the growth on non-planar substrate templates with complex surface topographies. Moreover, their one-dimensional structure allows electron diffraction from all parts of the surface when the electron beam is directed parallel to the stripes. This does not apply for two-dimensional patterns due to shadowing effects. In the present work, RHEED is employed to study the pattern evolution during buffer growth from multifaceted “U”- to single-faceted “V”-shaped stripes in real time, by which a high reproducibility of the pattern structure is achieved. Real-time monitoring was also applied during subsequent Ge growth at different substrate temperatures, revealing the critical coverages for sidewall ripple formation and 3D island nucleation. To obtain a real space picture of the nucleation process, the epitaxial surfaces were imaged in a step-wise manner using STM, where due to UHV conditions, epitaxial growth could be continued after each imaging step. In this way, a detailed microscopic picture of the island nucleation process is obtained.

Experimental

The investigations were carried out in a multichamber Si/Ge molecular beam epitaxy and scanning tunneling microscopy system equipped with a Si e-beam evaporator, Ge effusion cell, and an Omicron variable temperature STM. Stripe-patterned Si (001) substrates were produced by holographic lithography and CF_4 reactive ion etching. The stripes were aligned along the [110] surface direction and have a lateral period 350 nm and a depth of 40–50 nm as determined by atomic force microscopy. After standard RCA cleaning (see e.g. [20]), the native oxide was chemically removed by an HF dip, producing a stable hydrogen-passivated Si surface. The samples were then loaded into the MBE system and outgassed and annealed for 15 min at 750°C.

A two-step buffer Si growth procedure was employed to remove the processing defects and residual surface contamination. It consisted of a first low-temperature Si buffer layer of 25 nm thickness grown at a temperature of 450°C, followed by a second Si buffer growth at 520°C. After a short annealing at 600°C for 5 min, Ge was then deposited up to a thickness of 7 monolayers (ML) at two different

growth temperatures of $T_s = 520$ and 600°C. The Si and Ge growth rates were 2 and 1.5 Å/min, respectively, as checked by quartz microbalance as well as RHEED intensity oscillations. RHEED analysis was done using 25 kV electrons directed parallel to the stripes along the [110] azimuth direction. The intensity evolution of various diffraction spots as a function of deposited layer thickness was measured using a video-based image processing system. For STM investigations, the samples were rapidly quenched at different stages of growth with a rate of -10°C/sec , and then transferred under UHV to the attached STM chamber. Imaging was performed at tunneling currents of around 0.1 nA and applied sample bias of 2–4 V. Due to the low system pressure in the 10^{-11} mbar regime, growth could be continued afterward after a short annealing for a few minutes at 450°C.

Results

After patterning, the stripes exhibit a nearly rectangular geometry with vertical sidewalls and a depth of 40–50 nm [6]. Due to the surface roughness, etching defects, and residual carbon surface contamination, a spotty RHEED pattern is observed after hydrogen desorption and annealing, as shown by Fig. 1a. During Si buffer growth, the RHEED patterns rapidly evolve as illustrated by the sequence of diffraction patterns displayed in Fig. 1b–f. Already after 5 nm Si deposition at 450°C, the surface quality drastically improves and the initial 3D diffraction spots completely disappear (see Fig. 1b). Continuation of buffer growth, results in the appearance of faint additional diffraction streaks inclined by 25° to the surface normal, as indicated by the dashed lines in the RHEED pattern of Fig. 1c recorded after 10 nm Si growth. These diffraction streaks arise from electrons specularly reflected from the tilted sidewalls of the stripes. As illustrated schematically in Fig. 2, the tilt angle α of these streaks with respect to the (001) specular spot corresponds exactly to the sidewall tilt angle on the pattern surface. Their appearance thus indicates a rapid flattening of the sidewall surfaces and a preferential orientation toward {113} surface facets, which are inclined exactly by 25.4° to the (001) substrate orientation. Further Si growth at 450°C up to 25 nm (see Fig. 1d) does not change much the diffractions pattern.

Increasing the buffer growth temperature at this point to 520°C results in a rapid change in the RHEED patterns. After 2 nm further Si growth (Fig. 1e), the {113} facet spots sharpen and strongly increase in intensity. This indicates an initial rapid expansion, *i.e.*, growth of the {113} sidewall facets of the stripes. During further Si growth at 520°C, however, the {113} RHEED spots weaken again and new facet spots near the specular spot

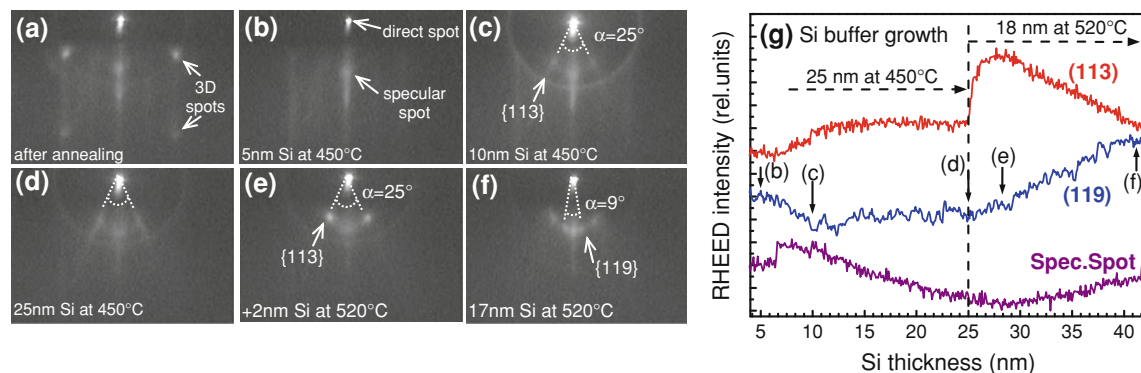


Fig. 1 Left: RHEED patterns during two-step Si buffer layer growth on stripe-patterned Si substrates recorded after 0, 5, 10, and 35 nm Si growth at 450°C and subsequent 2 and 17 nm Si growth at 520°C from (a) to (f), respectively. The {113} and {119} facet spots, as well as the corresponding sidewall inclination angle α (see schematic illustration of Fig. 2) are marked by the arrows and dashed lines.

Right: Normalized intensity evolution of the specular spot (purple), the {113} (red), and {119} (blue) facet spots arising from the sidewalls of the stripes plotted as a function of the Si buffer thickness. At 25 nm Si deposition, the substrate temperature increased from 450 to 520°C

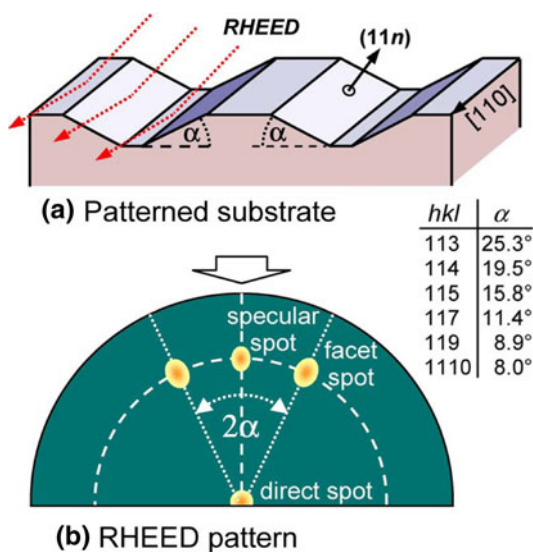


Fig. 2 Schematic illustration of the stripe geometry **a** as well as of the corresponding RHEED patterns **b** developed during buffer growth. Due to the {11n} sidewall facettation of the stripes with an inclination α relative to the in plane [110] direction, facet spots appear in the RHEED patterns that are tilted by α with respect to the specular spot

appear at a tilt angle of only about 9°, as indicated by the arrow in the RHEED patterns depicted in Fig. 1f after 17 nm Si deposition. The 9° tilt angle corresponding to a sidewall facet orientational near {119}, meaning that during the high-temperature buffer growth step, the sidewall inclination rapidly decreases due to surface mass transport toward the bottom of the stripes.

This observation is corroborated by the STM images presented in Fig. 3a and b that show the pattern structure after 7 nm, respectively, 20 nm Si buffer growth at 520°C. After 7 nm, the stripes assume a multifaceted “U”-shaped geometry, consisting of segmented sidewalls with main

{113}, {114}, and {119} facet orientations as indicated in Fig. 3a. The corresponding facet spots also appear in the surface orientation map (SOM) of the STM image depicted as insert. In these SOMs, the intensity of each spot represents the relative amount of surface area within the STM image with an $\{hkl\}$ orientation defined by the position (distance and azimuth angle) of the spot relative to the central (001) spot. Obviously, at 7 nm Si buffer, the {113} facet is most pronounced, in agreement with the RHEED data. The formation of {113} sidewall facets also agrees with the fact that the {113} surfaces have been found to be one of the major low-energy surfaces of silicon [21, 22], meaning that the sidewall facettation leads to a lowering of the total surface energy of the system. After 20 nm Si growth, however, the stripe morphology has changed to a shallow “V”-shaped form with an average sidewall inclination close to 9° as revealed by the corresponding STM image and surface orientation map shown in Fig. 2b. This transformation to mainly {119} oriented sidewalls is accompanied by a shrinking of the stripe depth from 35 to 7 nm after 20 nm Si growth. It is noted that the {119} facet spots in the surface orientation map are rather broad and elongated. This means that the sidewall orientation of the “V” stripes is not precisely defined, which explains the diffuse appearance of these facet spots in the corresponding RHEED pattern (Fig. 1f).

The change of stripe morphology during Si buffer growth is also reflected in the intensity evolution of the different RHEED diffraction features as a function of deposited Si thickness. This evolution is shown in Fig. 1g for the specular, as well as the {113} and {119} facet spots that are indicated by arrows in the RHEED patterns. The intensity of the specular spot (purple line) slightly increases during the first 4 nm low-temperature buffer growth (not shown), but then gradually decreases due to the rounding of

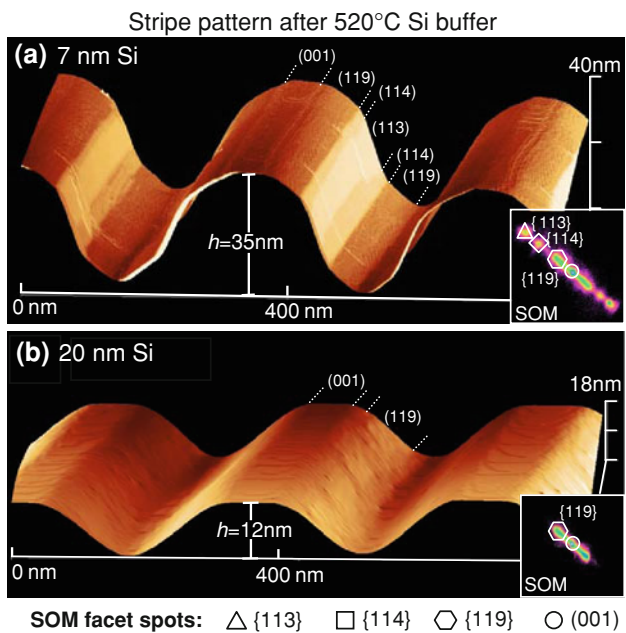


Fig. 3 STM images of the surface evolution of the stripe-patterned Si substrates during the second Si buffer growth step at 520°C at a buffer thickness of **a** 7 and **b** 20 nm, showing the transition from multifaceted “U”-shaped stripes with predominant {113} sidewall facets to shallower single-faceted “V”-shaped stripes, respectively. This is accompanied by a decrease in the height of the stripes from 35 to 12 nm. The inserts show the surface orientation maps (SOM) of the STM images, in which the *bright spots* indicate the most pronounced surface orientations of the pattern morphology. The different corresponding surface orientations are indicated by the *different symbols* as depicted below

the ridges and filling of the grooves (see STM image of Fig. 3), which decreases the amount of (001) surface area on the stripes. Toward the end of buffer growth at 520°C, however, the specular spot intensity increases again as the surface starts to planarize. The {113} facet spot in the RHEED patterns, for which the intensity evolution is depicted as red line in Fig. 1g, first appears after 10 nm low-temperature buffer growth, and its intensity abruptly increases when the substrate temperature is raised to 520°C during the second buffer growth step. It reaches a maximum after 3 nm Si growth, where the {113} sidewall facets are most pronounced. Further Si growth subsequently leads to a reduction in the (113) intensity and the (119) facet intensity (blue line in Fig. 1g) starts to rise as the multifaceted “U” stripes are transformed to “V”-shaped stripes. Termination of the Si buffer growth at this point yields well-defined stripe profiles with reproducible “V” geometry.

Ge growth on these “V” stripes was studied in a subsequent set of experiments. In the first set, Ge was grown at the same temperature as the second buffer at $T_s = 520^\circ\text{C}$. Figure 4a–f shows the sequence of RHEED patterns observed for Ge coverages increasing from 0 to 7 ML. The

corresponding intensity evolution of the specular spot and other diffraction features are shown in Fig. 4g on the right hand side. During the first 2 ML Ge deposition (see Fig. 4b), the RHEED pattern significantly changes, i.e., the residues of the {113} facet spots completely disappear and the specular spot intensity strongly decreases (purple line in Fig. 4g). The latter is caused by the surface roughening of the 2D Ge wetting layer surface associated with the formation of a high density of dimer vacancy lines and subsequently missing dimer rows [6, 19] in the surface reconstruction, which allows a partial stress relaxation [19]. As shown by our previous STM investigations [6], at 2 ML corresponding (2 × 8) surface reconstruction and a stable {11 10}, sidewall facet is formed with a slightly reduced inclination angle of 8° compared to 9° for the {119} facet. During further Ge deposition up to 4 ML, the RHEED patterns do not change much as shown by Fig. 4c. Beyond 4.2 ML coverage, however, splitted 3D diffraction spots appear in the RHEED patterns as indicated by the dashed squares in Fig. 4d and f, signifying the nucleation of 3D structures on the surface. From the measured intensity evolution versus coverage represented by the blue line in Fig. 4g, the critical thickness for the onset of this roughening transition is determined as 4.1 ML.

The surface structure formed in this roughening transition is revealed by the STM images displayed in row of Fig. 5 recorded after 4.5, 5.1, and 7 ML Ge growth. Already at 4.5 ML coverage (Fig. 5a), the STM image shows that the {11 10} sidewalls of the stripes are fully covered by ripples oriented perpendicularly to the [110] stripe direction. The ripples consist of alternating {105} microfacets, which is proven by the corresponding surface orientation map shown as insert. The average ripple height amounts to 9.3 Å, which is about twice of the deposited Ge thickness. Comparing RHEED and STM data, the extra RHEED diffraction spots appearing at this coverage can be directly assigned to this ripple formation, and the splitting of these diffraction spots is explained by the fact that the ripples on opposite sidewalls are tilted by 16° (=2 × 8°) with respect to each other. At 5.1 ML Ge coverage (Fig. 5b), additional pyramids and hut islands with {105} sidewall facets start to nucleate on the ridges of the stripes, and their density subsequently increases such that at 7 ML coverage (Fig. 5c), the ridges are decorated by these islands. At the same time, a coarsening and thickening of ripples on the sidewalls occurs. This is in contrast to the expected Ge accumulation at the bottom of the grooves, indicating that there is only little lateral redistribution of the deposited Ge adatoms. Thus, at 520°C, lateral Ge mass transport is inhibited due to slow surface diffusion. Moreover, the nucleation of Ge islands at the edges of the ridges indicates that there is an additional hopping barrier at the edges between the ridges and the sidewall facets.

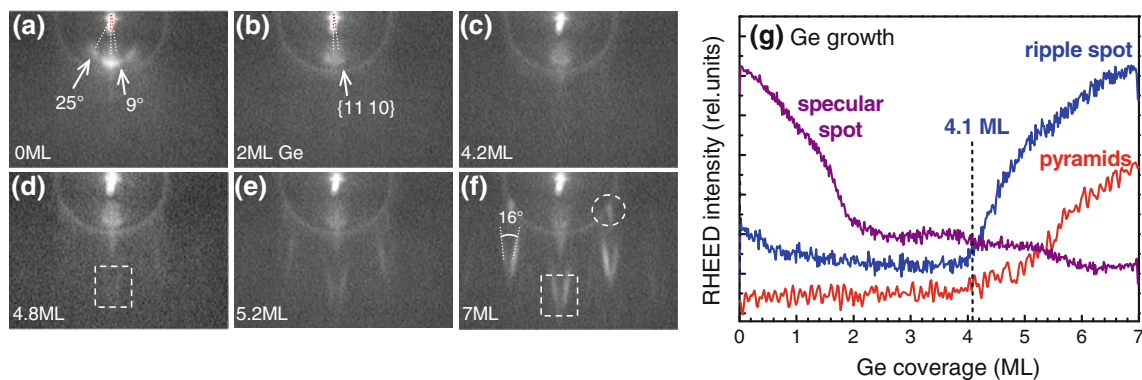


Fig. 4 Left: RHEED patterns recorded during Ge growth at 520°C on the stripe-patterned Si substrates at Ge thicknesses of 0, 2, 4.2, 4.8, and 7 ML from (a) to (f), respectively. Ripple formation on the surface results in the appearance of V-shaped diffraction spots as indicated in (f) by the dashed square. Before Ge growth, 45 nm Si was deposited, resulting in a “V”-shaped stripe geometry as shown in

Fig. 2b. Right: Panel g shows the normalized RHEED intensity evolution of the specular spot and two 3D diffraction spots indicated by the dashed square and circle in (f) as a function of Ge coverage. Accordingly, an onset of ripple formation and at a critical coverage of 4.1 ML is found

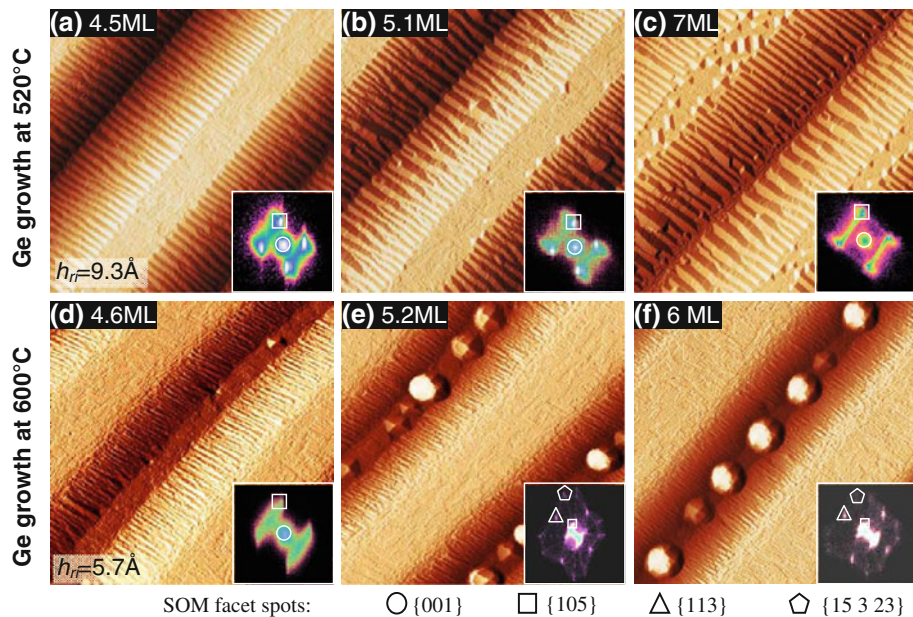


Fig. 5 Successive Ge growth on patterned Si substrates with “V”-shaped stripes for two different substrate temperatures of $T_s = 520^\circ\text{C}$ (top) and 600°C (bottom) as seen by STM ($500 \times 500 \text{ nm}^2$ images). The Ge coverage increases from 4.5 ML on the left hand side where sidewall ripple formation starts, to 5.1 ML in the middle, to finally to 6 ML, respectively, 7 ML on the right hand side. The average ripple

height at 4.5 ML coverage is $9.3 \pm 0.5 \text{ \AA}$ at 520°C and $5.7 \pm 0.5 \text{ \AA}$ at 600°C . Dome islands are only formed at the higher growth temperature and are aligned at the bottom of the grooves. The surface orientation maps of the STM images are shown as insets in which the observed $\{001\}$, $\{105\}$, $\{113\}$, and $\{15\ 3\ 23\}$ facet spots are indicated by the symbols

A completely different Ge island formation process occurs when Ge growth is performed at a higher temperature of 600°C , for which the corresponding RHEED patterns and intensity evolution of diffraction spots are shown in Fig. 6. Like for the case of 520°C growth, within the first two monolayers of Ge deposition the specular spot intensity strongly decreases due to the transition from the initial Si (2 × 1) to the Ge (2 × 8) surface reconstruction [6, 19], and any remnants of the tilted $\{113\}$ facet streaks in

RHEED disappear. Up to about 4 ML Ge, the surface structure and RHEED patterns remain practically unchanged (see Fig. 6b–c), and the splitted ripple diffraction spots only appear at a Ge coverage of 4.6 ML. This is also evidenced by the respective intensity versus Ge coverage curve depicted as blue line in Fig. 6g, where the abrupt intensity increase in the ripple spot at 4.6 ML is indicated by the vertical dashed line. Evidently, this onset is half a monolayer later than at the lower 520°C growth

temperature, and these ripple spots are obviously less sharp and pronounced. The corresponding STM image of the surface structure formed at 4.6 ML coverage is shown in Fig. 5d, evidencing indeed that the sidewall ripples at 600°C are smaller and less pronounced than those at 520°C (cf. Fig. 5a). According to STM line profiles measured along the sidewalls of the stripes, the average ripple height at 600°C is only 5.7 Å when compared to 9.3 Å at 520°C, indicating that at the higher growth temperature less material is incorporated at the sidewalls of the stripes.

At 5.2 ML Ge thickness, additional sharp diffraction spots appear in the RHEED patterns, as marked by the dashed circle in Fig. 6f. This signifies the formation of larger 3D islands on the epilayer surface. The onset is evidenced by the rapid intensity increase in these 3D diffraction spots at this coverage, as demonstrated by corresponding intensity evolution depicted as red line in Fig. 6g. At this coverage, pyramids as well as multifaceted dome islands are found the STM image depicted in Fig. 5e. The shapes of the Ge islands of pyramids and domes correspond exactly to those formed on unpatterned Si (001) surfaces. This is corroborated by the surface orientation map inserts in Fig. 5e–f, where the usual {105}, {113} and {15 3 23} facet spots of dome islands appear [23, 24]. Interestingly, at 600°C, the amplitude of the sidewall ripples does not increase at higher Ge coverages, which is an indication that the Ge thickness on the sidewalls does not increase much, because once formed practically all of the subsequently deposited Ge is transferred and incorporated into the 3D islands. This is substantiated by statistical analysis of the increase in the total island volume as a function of Ge coverage, which indicates that at 5.2 ML coverage already more than half a monolayer Ge is incorporated within the islands, assuming a Si/Ge intermixing of $x_{\text{Ge}} \sim 30\%$

within the domes as indicated by previous work (see e.g. [24]).

According to the STM images displayed in Fig. 5, at the higher growth temperature, Ge islands nucleate exclusively at the bottom of the grooves and they rapidly transform from pyramids to domes as growth proceeds. On the contrary, at low-temperature Ge islands form predominantly on the top of the ridges and retain their pyramidal shape even up to 7 ML coverage and only slowly grow in size. At 520°C, also the size of the sidewall ripple progressively increases with Ge coverage up to 7 ML, whereas the ripple amplitude quickly saturates at 600°C. These observations indicate a large lateral mass transport and material redistribution at the higher growth temperature, whereas it is only very small at 520°C, where lateral mass transport obviously only occurs on a very limited length scale. Indeed, at 520°C, the average island distance is only around 40 nm, compared to more than 350 nm (=lateral stripe period) at 600°C. The kinetically limited adatom diffusion at 520°C leads to nearly conformal wetting layer growth up to 4 ML Ge coverage. Thus, the critical coverage for island formation is reached simultaneously at the ridges and the sidewall surfaces, where 3D islands also form (see Fig. 5b). At 600°C, however, due to the higher adatom mobility, the capillary force arising from the high curvature at the bottom of the grooves [18] invokes a significant Ge downward mass transport. As a result, a flattening, i.e., filling of the bottom of the grooves occurs during Ge wetting layer growth as seen by STM in Fig. 5d and thus, also ripple formation is delayed. The Ge transfer to the bottom of the grooves leads to a local thickening of the Ge layer and thus to an exclusive Ge island nucleation at the bottom of the grooves. Once formed, nearly all additionally deposited Ge is sucked into these islands due

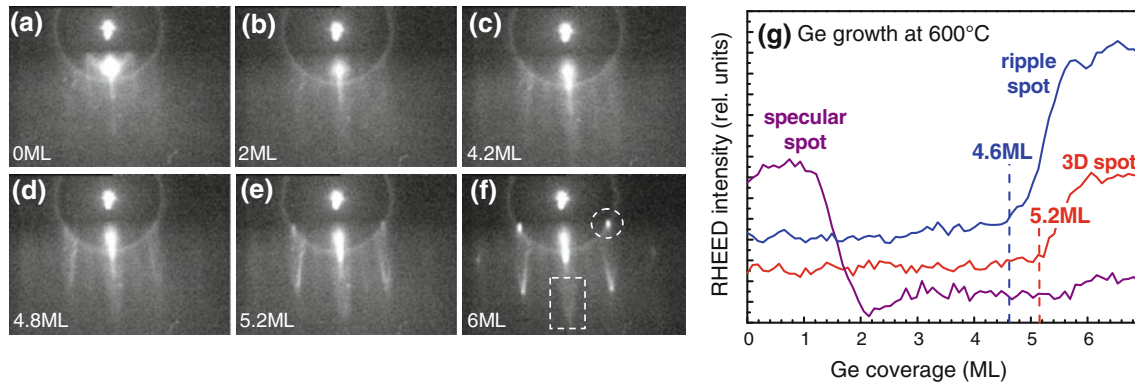


Fig. 6 Left: RHEED patterns observed during Ge growth at 600°C on stripe-patterned Si substrates with “V” geometry (see Fig. 2b) at Ge thicknesses of 0, 2, 4.2, 4.8, and 6 ML from (a) to (f), respectively. The onset of dome island formation at $\sim 5\text{ML}$ coverage is indicated by the appearance of 3D diffraction spots in the RHEED patterns (see dashed circle). Right: Intensity evolution as a function of coverage of

the specular spot, 3D ripple, and 3D island spot (purple, blue, and red line, respectively) indicated by the dashed square and circle in (f). As indicated by the vertical dashed lines, the onset of ripple formation occurs at a critical coverage of 4.6 ML, whereas dome nucleation sets in at critical coverage of 5 ML

to the large energy gain associated with the elastic strain relaxation. Therefore, STM images recorded at higher coverages show that even up to 11ML, no new islands are formed on any other surface location.

Conclusion

In this work, *in situ* RHEED monitoring of Si and Ge growth on stripe-patterned Si substrates was demonstrated as a sensitive tool for controlling the changes in the pattern structure as well as of the island formation process. This allowed to observe the transformation of the pattern geometry from multifaceted “U” to single-faceted “V” stripes. For subsequent Ge growth, ripple and island formation was observed by RHEED and STM, from which the onset of 3D islanding and sidewall roughening was precisely deduced. It was revealed that these processes significantly differ as a function of growth temperature, such that at 600°C ripple formation is significantly delayed compared to low-temperature growth at 520°C, whereas 3D islands starts slightly earlier. This is explained by the higher adatom mobility at the higher growth temperature, which leads to a substantial downward mass transport to the bottom of the grooves. As a result, site-controlled growth of Ge islands aligned in the bottom of the grooves can be obtained only at 600°C, whereas for lower temperatures islands nucleate randomly on the ridges as well as sidewalls of the stripes.

Acknowledgments The authors thank Alma Halilovic and Ursula Kainz for help with the holographic lithography and the Austrian Science Funds (SFB-IRON and P17436-N08) and the Gesellschaft für Mikro- und Nanoelektronik for financial support.

Open Access This article is distributed under the terms of the Creative Commons Attribution Noncommercial License which permits any noncommercial use, distribution, and reproduction in any medium, provided the original author(s) and source are credited.

References

- T.I. Kamins, R.S. Williams, *Appl. Phys. Lett.* **71**, 1201 (1997)
- T. Schwarz-Selinger, Y.L. Foo, D.G. Cahill, J.E. Greene, *Phys. Rev. B* **65**, 125317 (2002)
- J.J. Zhang, M. Stoffel, A. Rastelli, O.G. Schmidt, V. Jovanovic, L.K. Nanver, *Appl. Phys. Lett.* **91**, 173115 (2007)
- Z. Zhong, A. Halilovic, M. Mühlberger, F. Schäffler, G. Bauer, *J. Appl. Phys.* **93**, 6258 (2003)
- D.G. Matei, B. Sanduijav, G. Chen, G. Hesser, G. Springholz, *J. Crys. Growth* **311**, 2220 (2009)
- B. Sanduijav, D.G. Matei, G. Chen, G. Springholz, *Phys. Rev. B* **80**, 125329 (2009)
- Z. Zhong, P. Chen, Z. Jiang, G. Bauer, *Appl. Phys. Lett.* **93**, 043106 (2008)
- Z. Zhong, O.G. Schmidt, G. Bauer, *Appl. Phys. Lett.* **87**, 133111 (2005)
- G. Chen, H. Lichtenberger, G. Bauer, W. Jantsch, F. Schäffler, *Phys. Rev. B* **74**, 035302 (2006)
- G. Chen, G. Vastola, H. Lichtenberger, D. Pachinger, G. Bauer, W. Jantsch, F. Schäffler, L. Miglio, *Appl. Phys. Lett.* **92**, 113106 (2008)
- M. Grydlik, M. Brehm, F. Hackl, H. Groiss, T. Fromherz, F. Schäffler, G. Bauer, *New J. Phys.* **12**, 063002 (2010)
- J.L. Gray, R. Hull, J.A. Floro, *J. Appl. Phys.* **100**, 084312 (2006)
- A. Karmous, I. Berbezier, A. Ronda, R. Hull, J. Graham, *Surf. Sci.* **601**, 2769 (2007)
- I. Berbezier, A. Ronda, *Surf. Sci. Rep.* **64**, 47 (2009)
- C. Dais, H.H. Solak, Z. Ekinci, D. Grützmacher, *J. Appl. Phys. Lett.* **92**, 143102 (1998)
- T. Stoica, V. Shushunova, C. Dais, H. Solak, D. Grützmacher, *Nanotechnology* **18**, 455307 (2007)
- D. Kitayama, T. Yoichi, Y. Suda, *Thin Solid Films* **508**, 203 (2006)
- G. Biasiol, A. Gustafsson, K. Leifer, E. Kapon, *Phys. Rev. B* **65**, 205306 (2002)
- B. Voigtländer, *Surf. Sci. Rep.* **43**, 127 (2001)
- K.R. Reinhardt and W. Kern (eds.) *Handbook of Silicon Wafer Cleaning Technology*, (William Andrew Inc., 2007)
- A.A. Baski, S.C. Erwin, L.J. Whitman, *Surf. Sci.* **392**, 69 (1997)
- Z. Gai, R.G. Zhao, W. Li, Y. Fujikawa, T. Sakurai, W.S. Yang, *Phys. Rev. B* **64**, 125201 (2001)
- A. Rastelli, H. von Känel, *Surf. Sci.* **515**, L493 (2002)
- J. Stangl, V. Holy, G. Bauer, *Rev. Mod. Phys.* **76**, 725 (2004) and references therein